Excitation and Tuning of Higher-Order Fano Resonances in Plasmonic Oligomer Clusters

Daniel Dregely,[†] Mario Hentschel,[†,‡,*] and Harald Giessen[†]

[†]4th Physics Institute and Research Center SCoPE, University of Stuttgart, D-70569 Stuttgart, Germany, and [‡]Max Planck Institute for Solid State Research, Heisenbergstrasse 1, D-70569 Stuttgart, Germany

ABSTRACT Plasmonic oligomer clusters are assemblies of closely packed metallic nanoparticles. They provide a rich set of spectral features such as Fano lineshapes and a simultaneous tunability of the supported resonances in the optical wavelength regime. In this study, we investigate numerically and experimentally clusters of plasmonic nanoparticles that exhibit multiple Fano resonances due to the interference of one broad superradiant mode and multiple narrow subradiant modes. In particular we investigate oligomers with multiple ring modes and elongated chains of nanoparticles surrounded by one ring of nanoparticles. We show that the number of nanoparticles and their respective arrangement in the cluster strongly influence the spectral position and modulation depth of the spectral signature of the supported modes. Our study opens up the pathway to "plasmonic super molecules" that show unprecedented tunability, which renders them highly suitable for applications such as multiwavelength surface-enhanced Raman scattering.

KEYWORDS: plasmon hybridization · coupling · Fano resonances · dark mode · oligomer cluster

Artificial plasmonic molecules, consisting of individual nanoparticles that interact *via* their near-fields, have recently gained tremendous interest. Dimers,[1−5] trimers,[6] quadrumers,[7,8] and more complex arrangements, such as plasmonic oligomers,[9−11] show intriguing spectral features such as Fano resonances.[12−15]

Just like electronic wave functions in molecules mix and hybridize, forming new collective modes, the near-field interaction of particle plasmon resonances supported by metallic nanoparticles leads to the emergence of new collective plasmonic modes.[1,16] In order to deduce the nature of the modes in complex plasmonic oligomers, symmetry considerations are as important as group theory in molecular physics.[6,17−21] A plasmonic heptamer, consisting of one center particle surrounded by six ring particles, has D_{6h} spatial symmetry, leading to a bright superradiant and dark subradiant collective mode without the need of symmetry breaking in the structure. The spectral overlap and destructive interference of these two modes leads to the formation of an asymmetric Fano line shape in the scattering spectrum of the heptamer. It was recently shown that the formation of the collective mode is mediated by near-field coupling of the individual particles, rendering the shape of the Fano resonance crucially dependent on the interparticle distance.[10] Further tunability on the Fano resonance is gained by changing the dipole moment of the ring mode with respect to the dipole moment of the center particle, hence changing the remaining dipole moment of the subradiant mode and consequently the modulation depth of the resonance. A multitude of tuning parameters is possible, for example number, material, and size of particles. Additionally, structural tuning, *e.g.*, changing interparticle distances as well as symmetry breaking by leaving out or displacing certain particles, makes plasmonic oligomers highly interesting for sensing,[22−26] multiwavelength surface-enhanced Raman scattering (SERS),[27] multiwavelength surface-enhanced infrared absorption spectroscopy (SEIRA),[28] future photonic circuits,[29,30] or slow-light applications.[31]

In this article, we go beyond simple plasmonic heptamers. First, we investigate numerically and experimentally the spectral response of plasmonic oligomer structures with an added second outer ring of particles. As a consequence, the resulting plasmonic super molecules support additional or modified bright and dark modes. Those structures were theoretically proposed by Bao *et al.*, calculating the far-field extinction spectra of the structures.[32] We have fabricated the structures and measured extinction spectra. We identify the second occurring resonance as a second-order dark mode with near-field distributions that indicate antiphase oscillation of the two ring modes and the center particle.

* Address correspondence to m.hentschel@physik.uni-stuttgart.de.

Received for review July 29, 2011 and accepted August 31, 2011.

Published online August 31, 2011
10.1021/nn202876k

Second, we analyze an elongated chain of nanoparticles that is surrounded by a particle ring. In accordance with the structural symmetry, higher-order Fano resonances can be excited under normal incidence with the polarization of the incident light set perpendicular to the chain axis. The number of Fano resonances depends on the number of center particles and, therefore, on the length of the elongated particle chain. Strikingly, by removing certain particles from the ring, a tremendous tunability of the modulation depth of the resonances is observed, both theoretically as well as experimentally. Employing near-field calculations we identify the excited collective subradiant modes for the different oligomer chains. The fact that for polarization along the chain axis only a single Fano resonance is present allows switching on and off higher-order Fano resonances at will in these clusters.

In the quest for new plasmonic super molecules, we believe that our study conveys a deeper insight into the modes supported by these large nanoparticle clusters and offers tuning possibilities of the multiple Fano resonances.

RESULTS AND DISCUSSION

In Figure 1 we investigate the influence of adding a second outer particle ring to the heptamer configuration. The scanning electron micrographs show the heptamer and the two larger clusters belonging to the same symmetry group D_{6h}.[32] We have fabricated the structure using electron beam lithography and subsequent evaporation of gold on a glass substrate. The interparticle distance is 20 nm, and the height of the gold nanodisks is 80 nm. A good uniformity of the fabricated clusters, arranged in a $100 \times 100\,\mu m^2$ square lattice, is obtained, allowing for ensemble measurements of transmittance in a Fourier-transform infrared spectrometer. We compare the measured 1-transmittance spectra (left column in Figure 1) to calculated extinction spectra obtained with finite integration techniques (right column in Figure 1, for further technical details see Methods section).

The Fano dip in the heptamer spectrum (number of particles $N = 7$) resulting from the interference of the spectrally broad superradiant and the narrow subradiant mode is clearly visible (blue curve). The formation of the two collective modes is mediated *via* the plasmonic near-fields, leading to in-phase oscillations of all plasmonic nanoparticles (superradiant mode) and out-of-phase oscillation of the center particle and ring particles (subradiant mode). With increasing number of particles in the clusters ($N = 13$ and $N = 19$) the overall dipole moment of the superradiant mode increases, resulting in an increased radiative damping and thus a spectral broadening. In the experimental spectra just one Fano dip is observable (indicated by the black arrows), which gradually shifts to lower energies for the larger clusters. This results in a spectral detuning of superradiant and subradiant modes, which is nicely confirmed by simulations.

In simulations, besides the fundamental Fano dip, a second Fano resonance is present for the $N = 13$ and $N = 19$ clusters (red arrows). A second blue-shifted subradiant mode interferes with the broad superradiant mode. The modulation depth of this resonance is low, especially in the case of the $N = 19$ cluster, which makes it impossible to observe it experimentally in our system. Only a slight kink is visible in the experiments. Using single-crystalline instead of thermally evaporated gold would decrease the intrinsic damping in the material and lead to a better modulation of the Fano resonances.[33] Furthermore, decreasing the interparticle distance causes increased near-field coupling and hence more pronounced resonances.[10] Recent experiments show the realization of sub-10-nm gap sizes employing new fabrication processes.[34]

In order to explain the appearance of higher-order Fano resonances in the larger clusters, we plot the near-field distributions at the spectral positions of the Fano resonances in Figure 2. We use plane-wave incidence with linear polarization as shown in Figure 1. For the $N = 13$ and $N = 19$ clusters two ring modes are supported. Similarly to the heptamer case the particle plasmon mode of the center particle hybridizes with the ring mode of the adjacent six nanoparticles, giving rise to in-phase and out-of-phase collective modes. The outer ring, formed by the added nanoparticles, supports a second ring mode. From the electric near-field distribution at the Fano resonances we infer that hybridization of the outer ring mode with the dark mode of the heptamer configuration leads to a lower-energy first-order and higher-energy second-order dark mode. This corresponds to in-phase oscillation (top row in Figure 2) and out-of-phase oscillation of the two ring modes (bottom row in Figure 2). These two dark modes are shifted to lower and higher energy, respectively, due to attractive and repulsive near-field interaction. Due to its large overall dipole moment, the bright mode is spectrally very broad, hence overlapping with both supported dark modes that cause the two Fano dips.

By adding more particles to the outer ring ($N = 19$ *versus* $N = 13$ cluster) the first-order and second-order Fano resonances shift to lower energies, since the energy of the outer ring mode is lowered due to attractive electric dipole interaction between adjacent nanoparticles. Consequently, the hybridized first and second dark modes are lowered in energy, which results in a spectral red shift. Also, the line width of the first-order Fano dip increases and the modulation depth decreases for the larger cluster, which can again be understood by inspecting the field distributions. The net dipole moment in the $N = 13$ cluster at the first-order Fano resonance is lower than for the $N = 19$

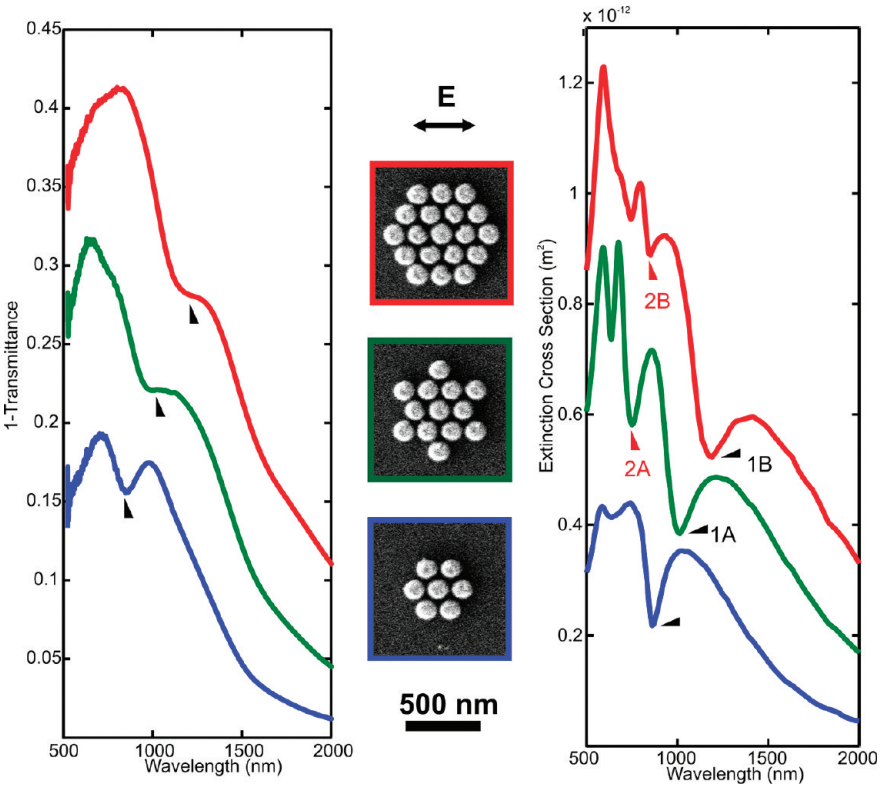

Figure 1. Experimental 1-transmittance spectra (left panel) and simulated extinction spectra (right panel) of the clusters (green and red curves) compared to the spectra of a heptamer (blue curves). By adding a second ring to the heptamer the clusters support a second-order Fano resonance (red arrows) as well as the fundamental Fano resonance (black arrows). Only the fundamental dark mode is well modulated in the experimental spectra. The labeling of the arrows in the simulated spectra indicates the spectral position of the respective field plots in Figure 2.

cluster, where the dipole moment of the in-phase oscillating ring particles dominates the out-of-phase dipole moment of the center particle.

On the high-energy side of the theory spectra we observe even higher-order excitations. At these energies quadrupolar-like charge distributions in the nanoparticles become important. These modes can no longer be easily understood in the dipolar model that we employed so far.

We have seen that the addition of nanoparticles to a heptamer leads to the formation of new collective modes that modify its spectrum. Another possibility to enlarge the clusters while keeping a high degree of structural symmetry is to elongate the cluster along one of its axes, or, to phrase it differently, surround a chain of center particles with a ring of outer particles. Therefore we add 3, 6, 9, and 12 nanoparticles to the heptamer configuration, hence elongating the cluster gradually in one direction. The structures are depicted in Figure 3. We calculate the extinction spectra for incident polarization along the two symmetry axes as shown in Figure 3.

For incident polarization along the long axes of the clusters (blue curves), no additional Fano dip arises with increasing chain length. Surprisingly, the Fano resonance shows only minor shifts in its spectral position by elongating the cluster. Hybridization of the ring mode and the center particle chain mode leads to the formation of a superradiant mode where all particle plasmons are in-phase and a subradiant mode where the center particle plasmons are out-of-phase with respect to the ring particle plasmons (see Figure 4). Interference of these modes leads to the asymmetric dip in the blue spectra. For the superradiant mode two spectral changes are observed for larger clusters. First, the width of the superradiant mode is significantly broadened since the sum of the dipole moments of all in-phase oscillating particle plasmons is increasing. Second, the mode shifts to lower energies as the attractive electric dipole forces increase with adding particles to the cluster.

When the incident light is polarized along the short axes of the clusters (green curves), higher-order Fano resonances are observed. In Figure 3 we label them with arrows and denote them as first (black arrows), second (red arrows), and third (blue arrows) order. The spectral position of the same-order Fano dips is shifted to lower energies for increasing number of center particles. Compared to the perpendicular polarization, the superradiant mode is not significantly broadened and no energy shift is observed, indicating that radiation damping and coupling forces in the collective bright mode are not largely altered for incident polarization along the short axes of the plasmonic oligomer

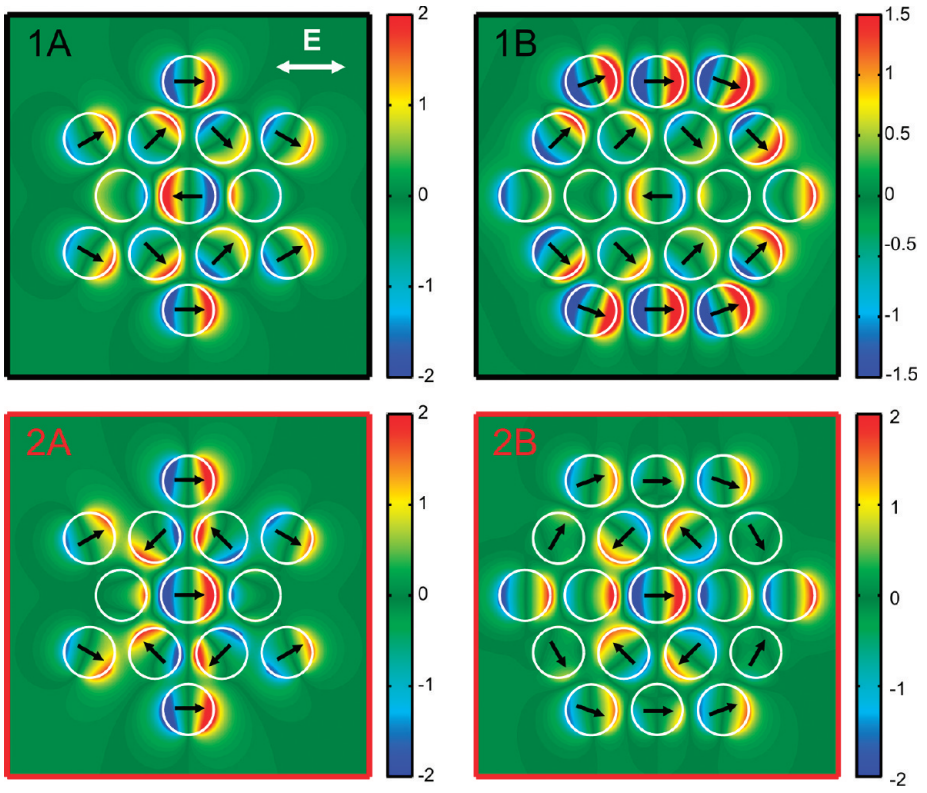

Figure 2. Simulated electric near-field distributions (E-field component perpendicular to the substrate plane normalized to the amplitude of the incident plane wave) of the fundamental dark modes (black boxes) and the second-order dark modes (red boxes). The spectral positions are indicated by the arrows in Figure 1. For all cases the center particle oscillates out-of-phase with the adjacent particles building up the inner ring. For the second-order dark mode also the outer ring oscillates out-of-phase with respect to the inner ring, which is not the case for the fundamental mode where all ring particles oscillate in-phase.

clusters. It is noteworthy that an additional Fano resonance is observed only if the number of center particles is uneven. In the case of the heptamer and the cluster with two center particles, only one Fano dip is present, whereas for the clusters with three center particles a second Fano dip is formed, and for five center particles even a third Fano dip is observed. The first- and second-order dark modes are increasingly detuned from the bright mode in larger clusters, which makes the fundamental Fano dip barely visible in this case.

The difference in geometry of the clusters along their two symmetry axes causes a pronounced anisotropy in the spectral response. Depending on the polarization direction, it is possible to switch Fano resonances on and off within the spectrum of the same plasmonic system.

In order to analyze the underlying physics of the spectral features in the chain clusters, we extract the vertical electric field component from near-field simulations with the polarization of incident light set along the short axes of the clusters. The dark mode near-field distributions of the clusters with three, four, and five center particles are plotted in Figure 5A, B, and C. To comprehend the appearance of higher-order Fano resonances, we have to consider the spatial symmetry of the elongated oligomer cluster. With the incident polarization set along the short axes of the clusters the vertical field components and charge distributions have to mimic the structural symmetry as well. Therefore, by adding one center particle to the cluster with three center particles in Figure 5A no additional dark mode is supported by the structure. From a symmetry viewpoint the two outer particles are identical and need to have identical charge distributions, which similarly holds true for the two center particles. Hence, only the two dark modes with the charge distributions depicted in Figure 5B are observed. An analogous symmetry argument holds for the two center particle cluster, which supports only the fundamental dark mode.

In the case of the cluster with three center particles at the spectral position of the Fano resonances (Figure 5A) the three center particles oscillate out-of-phase with respect to each other. The low-energy fundamental dark mode is an in-phase oscillation of this mode supported by the center particles with the ring mode, whereas the ring mode oscillates out-of-phase for the high-energy second dark mode. The higher attractive forces in the case of the in-phase oscillation of the ring mode and the mode supported by the center particles (first dark mode) lead to a lowering of energy when compared to the

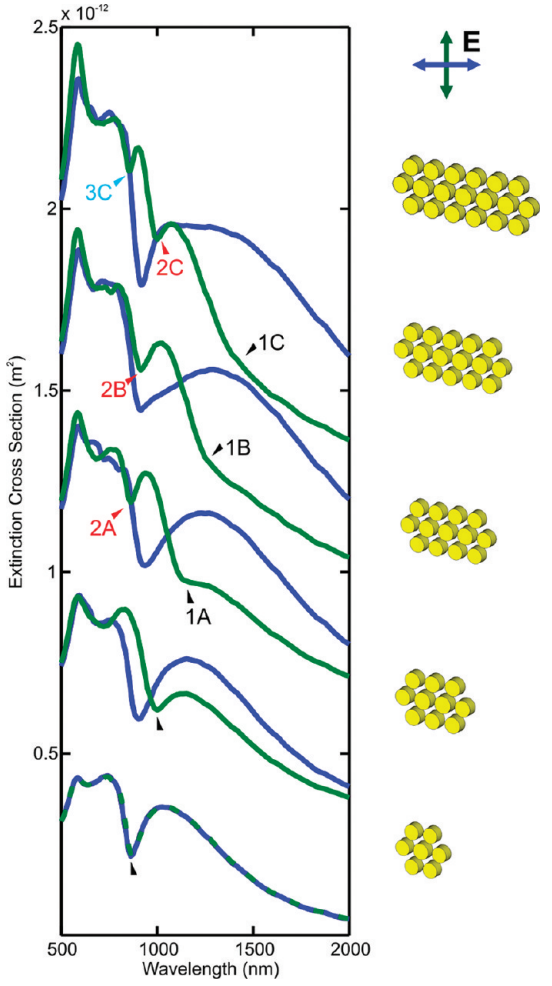

Figure 3. Simulated extinction spectra of the elongated oligomers for horizontal (blue curves) and vertical (green curves) incident polarization. The spectra are shifted for clarity by an offset. For vertical polarization, with increasing number of particles the elongated oligomers support besides the fundamental dark mode (black arrows) higher-order dark modes (second- and third-order dark modes indicated by red arrows and blue arrow, respectively). Changing the polarization can switch on or off and tune the spectral position of the narrow Fano resonances. The labeling of the arrows indicates the spectral position of the respective field plots in Figure 5. For horizontal polarization higher-order subradiant modes are not observed.

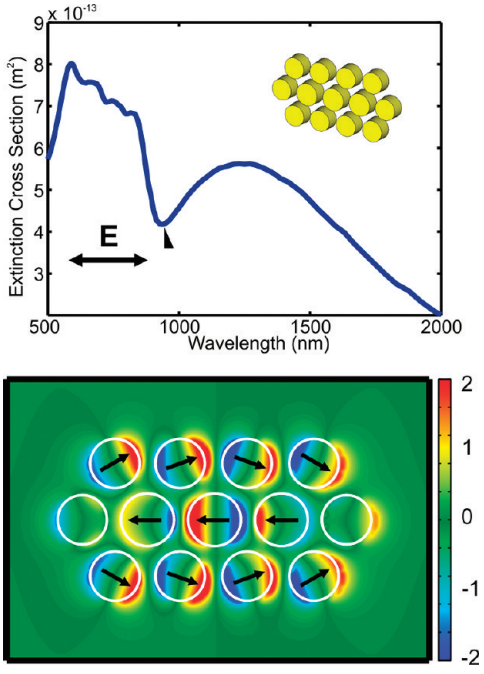

Figure 4. Simulated extinction spectrum of the elongated oligomer with three center particles for horizontal incident polarization. The black arrow indicates the spectral position of the calculated near-field distribution at the Fano resonance. The center particle plasmons are out-of-phase with respect to the ring particle plasmons. Only the fundamental dark mode is supported for horizontal polarization. Similar field distributions are obtained at the Fano resonance for the oligomers with two, four, and five center particles.

out-of-phase oscillation in the case of the second dark mode. The situation is similar for the cluster with four center particles (Figure 5B). There, due to mirror symmetry, the two innermost center particles form a synchronous pair that oscillates out-of-phase with respect to the next left and right middle row particle. Again, hybridization of this mode with the outer ring mode results in the formation of a fundamental and a second-order dark mode. The situation changes by adding a fifth center particle. In Figure 5C, the field distributions of the three dark modes are depicted. In the first- and second-order mode the two left and two right middle row particles pair and oscillate out-of-phase with respect to the center particle. This mode hybridizes with the outer ring mode and results in the two collective dark modes shifted to lower and higher energy due to attractive and repulsive near-field interaction. At the spectral position of the third-order mode, the mode supported by the center particles is an out-of-phase oscillation of all particles with respect to each other. It is remarkable that an antisymmetric oscillation in the laterally aligned center particle chain can be excited without breaking the symmetry and introducing any retardation into the system.

In the electric near-field distributions we observe that the contribution to the overall ring dipole moment is dominated by the three left- and three rightmost ring particles. The residual ring particles are only weakly contributing to the formation of the collective dark modes. Therefore, in the following we consider plasmonic oligomers where we leave out the residual ring particles. This strategy opens up the possibility to increase the modulation depth and to shift the spectral position of the narrow Fano resonances.

In Figure 6 we compare the spectra of the elongated chain oligomers (green curves) with the oligomer clusters where we remove the upper and lower ring particles (red curves). The modulation depth of the low-energy Fano resonance is very poor. It shifts to the red upon increasing the number of center particles and vanishes completely for the large cluster with four central nanoparticles. Strikingly, the second Fano

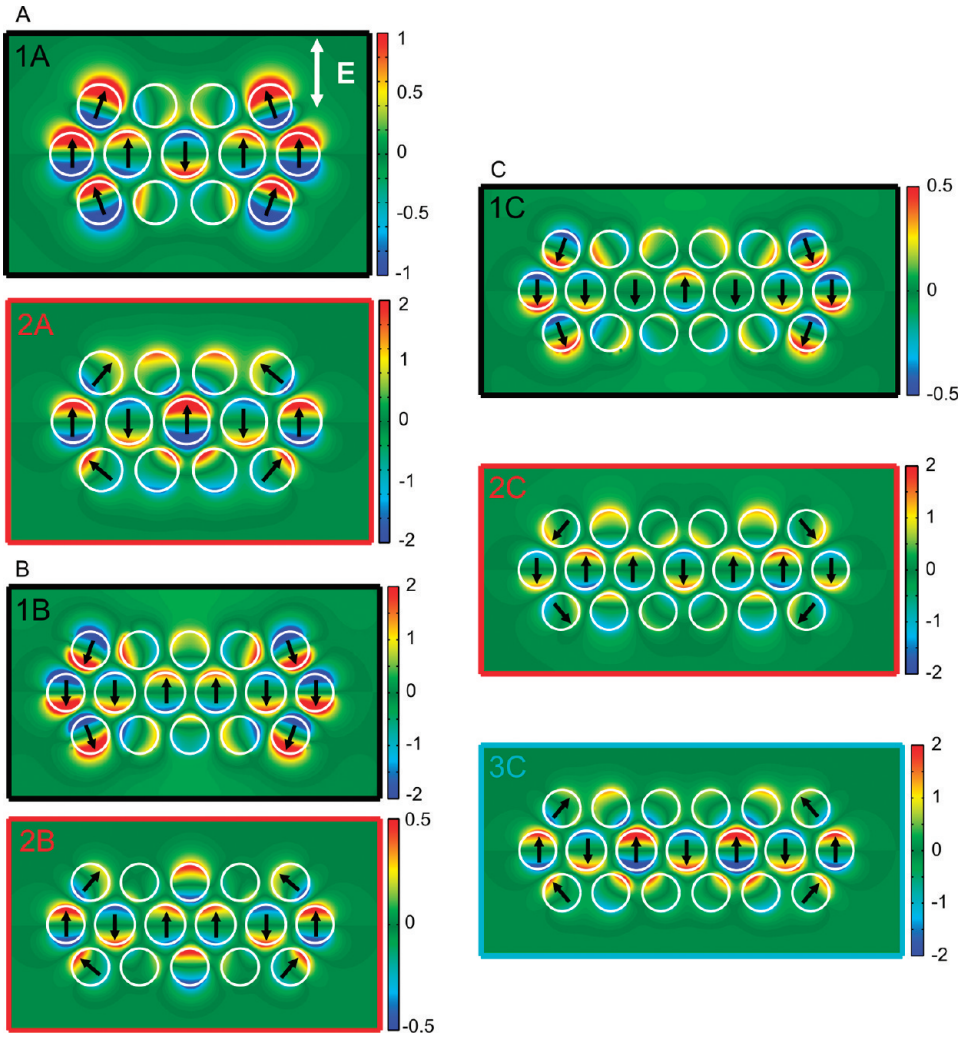

Figure 5. Simulated near-field distributions of the elongated oligomers for vertical polarization at the spectral positions labeled in Figure 3. Oligomers with (A) three center particles and (B) four center particles supporting fundamental (1A and 1B) and second-order (2A and 2B) subradiant modes. (C) Oligomer with five center particles exhibits three subradiant modes.

resonance that first appears for the cluster with three center particles is strongly modulated compared to the oligomer chain cluster. Good cancellation of the net dipole moment and spectral overlap of dark and bright mode is achieved in this case. Furthermore the Fano dip is shifted to higher energies by removing ring particles compared to the Fano feature in the plasmonic chain oligomer. This behavior is also observed for the cluster with four center particles, though the second-order Fano resonance is broadened compared to the three center particle cluster.

In Figure 7 we plot the simulated spectrum and near-field distributions of the cluster with three center particles. The spectral positions of the first lower-energy and second higher-energy dark modes are indicated with a black and red arrow, respectively. The excited modes are similar to the two dark modes of the elongated chain cluster with all ring particles (see Figure 5A), resulting from hybridization of the ring particle mode with the center particles mode. Energetically, the two modes are shifted to higher energies by removing ring particles. This is due to less attractive interaction *via* near-field coupling between the plasmonic nanoparticles. The spectral feature of the first-order dark mode is nearly absent in the spectrum. The eight in-phase oscillating particles create a dipole moment that is only very weakly reduced by the out-of-phase oscillation of the center particle, which makes the dipole moment comparable to the dipole moment of the bright mode. Therefore, an asymmetric dip in the spectrum is barely visible at this energy. In the case of the unchanged chain oligomers the additional particles in the ring further reduce the dipole moment (*cf.* the field distribution of Figure 5A), leading to the Fano dip in the green spectrum. Yet, a very pronounced modulation of the second-order Fano resonance is achieved by removing these upper and lower ring particles. This is due to a very efficient reduction of the net dipole moment in this particle configuration at this energy. Comparing the electric

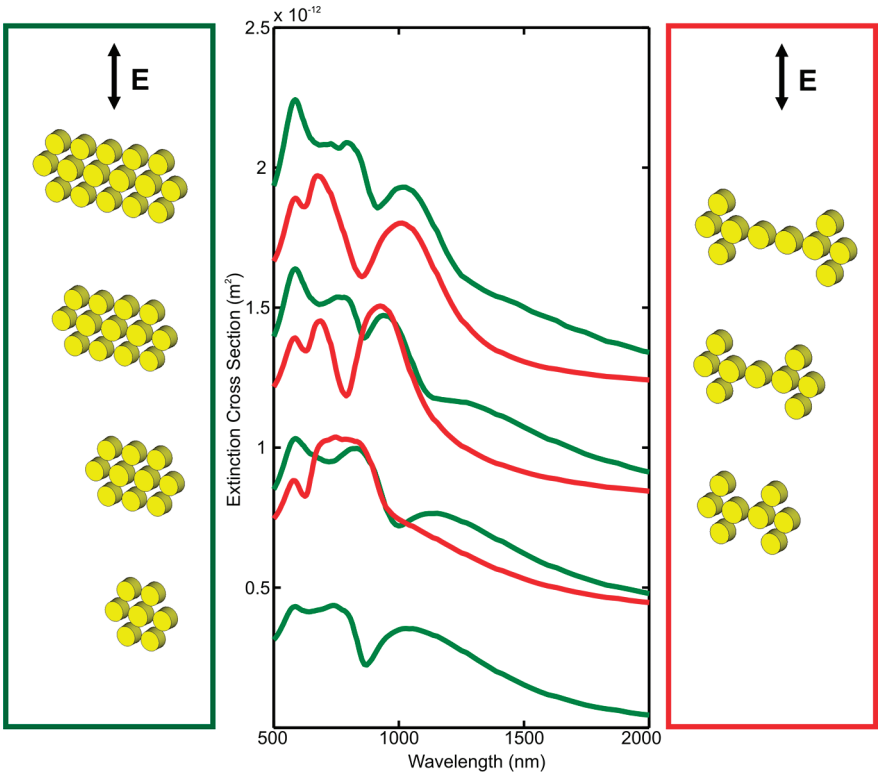

Figure 6. Simulated extinction spectra for elongated oligomers with removed ring particles compared to extinction spectra of the chain oligomers. Leaving out certain ring particles leads to higher modulation depth of the Fano resonance in the extinction spectra (red curves) than for the elongated oligomers (green curves). Also, the spectral position is shifted to shorter wavelengths.

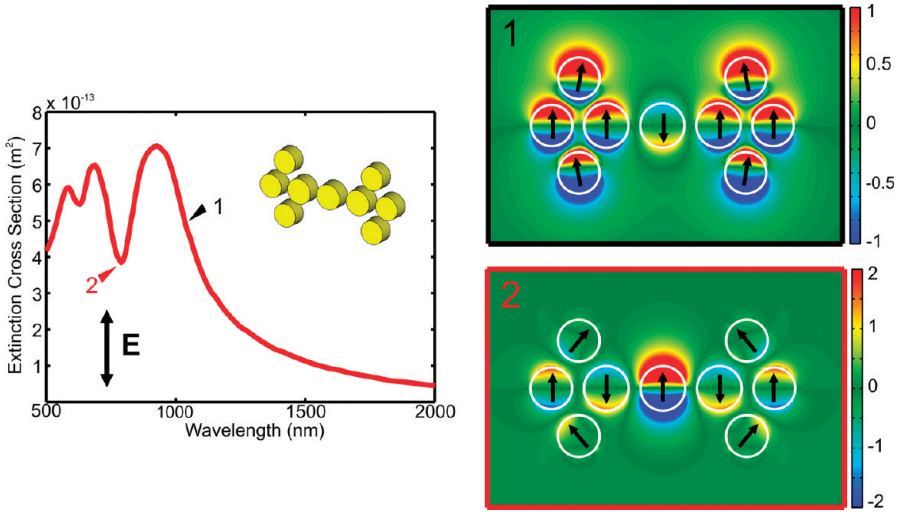

Figure 7. Electric near-field distribution of the oligomer with three center particles and missing ring particles. The spectral positions are labeled in the extinction spectrum. The second-order subradiant mode is very pronounced since the overall dipole moment of the in-phase and the overall dipole moment of the out-of-phase oscillating particles are matched. Contrarily, the first-order dark mode is barely visible in the spectrum since the absolute dipole moment of the outer particles is overdominating the out-of-phase dipole moment of the center particle.

near-fields of the second-order dark mode in Figure 7 with the field distribution in Figure 5A, we deduce that the additional ring particles tend to increase the overall dipole moment, which explains the lower modulation depth of the Fano dip in the green curve compared to the Fano dip in the red curve of Figure 6. Hence, leaving out certain ring particles leads to a shift in energy of the Fano resonances and a tremendous increase of the modulation depth of the second-order Fano resonance. We also would like to point out that by adding one particle to the two-center particle cluster a narrow extinction dip at 800 nm opens up in the previously broad extinction peak.

We have fabricated a series of clusters and compare them to the oligomer spectrum with the polarization set along the short axes of the clusters. The experimental results are shown in Figure 8. The fundamental dark mode is observed only in the heptamer spectrum (blue curve) due to dipole moment mismatch of in-phase and out-of-phase oscillating nanoparticles and energy detuning of bright and dark modes in the case of the bigger clusters. Symmetry forbids the existence of a second dark mode for the cluster with two center particles. In the case of three center particles we identify the Fano line shape as the second-order dark mode since it is clearly shifted to higher energies, when compared with the Fano resonance in the heptamer. Adding a further center particle shifts the second dark mode to lower energies and decreases the modulation depth just as predicted by simulations (see Figure 6). Due to the reduction of the net dipole moment of the second dark mode in this cluster configuration, we can now clearly observe experimentally the higher-order Fano resonance in our oligomer clusters.

CONCLUSIONS

In this article we studied theoretically and experimentally the appearance and properties of higher-order Fano resonances in large oligomer clusters. Calculating the near-field distribution allowed us to observe the hybridization of a second ring mode with the dark mode in a plasmonic heptamer, leading to the occurrence of a higher-order Fano resonance. Furthermore, we investigated plasmonic structures where we elongated the heptamers in one direction by adding additional center particles. When the incident polarization was set along the short axes of the clusters, higher-order Fano resonances up to a third-order dark mode were observed. In that case, due to the structural symmetry, an additional dark mode was observed only if the number of center particles is uneven. It is noteworthy that by changing the incident polarization by 90° only the fundamental dark mode could be excited for all elongated plasmonic oligomers. This can be used in future applications to turn on and off spectrally narrow resonances. By leaving out certain ring particles we could tune the second-order Fano resonance in energy and likewise increase the modulation depth tremendously.

We demonstrated that such artificial plasmonic molecules provide high tuning possibilities on multiple sharp spectral features. This makes them very suitable for applications in plasmonic nanocircuits,[35,36] high-Q applications, such as nanolasers,[37] or strong coupling of quantum systems to nanocavities. With the electric fields at the Fano resonances being strongly enhanced in a deep subwavelength volume between the nanoparticles,[38] plasmonic oligomer clusters have a high potential to serve as platforms for multiwavelength surface-enhanced Raman scattering,[39] multiwavelength plasmonic sensing,[40] or higher-order harmonics generation.[41]

We believe that our study gives further understanding of complex plasmonic oligomer clusters and opens up the way to new structures with tremendous implications in material and life sciences.

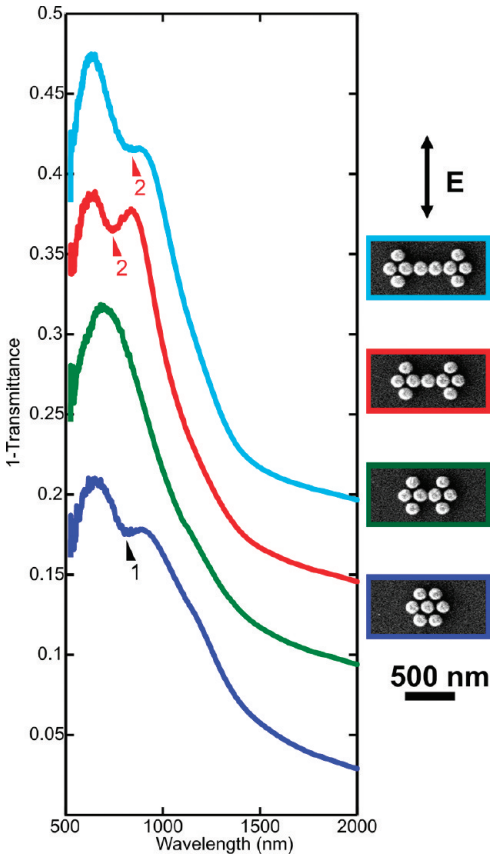

Figure 8. Experimental 1-transmittance spectra of the elongated oligomers with missing ring particles. Only the first-order subradiant mode is existent in the heptamer (blue curve) and the oligomer with two center particles (green curve). Adding one or two more particle leads to the formation of a second-order Fano resonance (red arrows in the red and cyan spectrum). The fundamental dark modes are not observable in the spectra due to dipole moment mismatch.

METHODS

We use finite integration techniques to calculate the extinction spectra and the near-field distributions at the respective spectral positions (CST Microwave Studio, Darmstadt, Germany). The dielectric function of gold was taken from measured data.[42] In order to account for the quartz substrate in the fabricated structure, the structure is embedded in a homogeneous background material with effective refractive index $n = 1.25$. Since only in-plane modes are studied, the assumption of a homogeneous medium is justified. For vertical modes the symmetry breaking due to the

quartz–air interface would significantly alter the optical modes, which is not the case for laterally polarized modes.

The structures are fabricated using electron-beam lithography (Raith e_Line) in a positive resist (PMMA) process. After electron exposure and development of the resist a 3 nm Cr adhesion layer and a 80 nm gold layer are evaporated. Subsequent lift-off removes the residual resist and metal. Each geometry is periodically arranged in a 100 × 100 μm^2 field. Exemplary structures are shown in the scanning electron micrographs of Figure 1 and Figure 8, taken with a Hitachi S-4800 scanning electron microscope. All ring particles have a diameter of 150 nm, and the center particles have a diameter of 160 nm. The height of the structures is 80 nm. The slight conical shape due to the lift-off procedure is taken into account in the simulations.

Extinction (1-transmittance) spectra are measured with a Fourier-transform infrared spectrometer (Bruker Vertex 80, tungsten lamp), equipped with an infrared microscope (Bruker Hyperion). The incident light was focused with a 15× Cassegrain objective with numerical aperture $N = 0.4$, and the transmitted intensities are detected with a liquid N_2-cooled MCT 77 K detector and a Si diode. The incident polarization was set with an infrared polarizer, and the measured spectra are normalized with respect to the bare quartz substrate.

Acknowledgment. D.D. and M.H. contributed equally to this work. D.D., M.H., and H.G. were financially supported by Deutsche Forschungsgemeinschaft (SPP1391 and FOR730), by BMBF (13N9048 and 13N10146), by Baden-Württemberg Stiftung, and by German-Israeli Foundation. D.D. additionally acknowledges support by the Carl-Zeiss-Stiftung.

REFERENCES AND NOTES

1. Nordlander, P.; Oubre, C.; Prodan, E.; Li, K.; Stockman, M. Plasmon Hybridization in Nanoparticle Dimers. *Nano Lett.* **2004**, *4*, 899–904.
2. Kim, D.-S.; Heo, J.; Ahn, S.-H.; Han, S. W.; Yun, W. S.; Kim, Z. H. Real-Space Mapping of the Strongly Coupled Plasmons of Nanoparticle Dimers. *Nano Lett.* **2009**, *9*, 3619–3625.
3. Rechberger, W. Optical Properties of Two Interacting Gold Nanoparticles. *Opt. Commun.* **2003**, *220*, 137–141.
4. Alù, A.; Engheta, N. Hertzian Plasmonic Nanodimer as an Efficient Optical Nanoantenna. *Phys. Rev. B* **2008**, *78*, 1–6.
5. Davis, T.; Vernon, K.; Gómez, D. Designing Plasmonic Systems Using Optical Coupling Between Nanoparticles. *Phys. Rev. B* **2009**, *79*, 46–48.
6. Brandl, D. W.; Mirin, N. A.; Nordlander, P. Plasmon Modes of Nanosphere Trimers and Quadrumers. *J. Phys. Chem. B* **2006**, *110*, 12302–12310.
7. Urzhumov, Y. A.; Shvets, G.; Fan, J. A.; Capasso, F.; Brandl, D.; Nordlander, P.; Plasmonic Nanoclusters, A Path Towards Negative-Index Metafluids. *Opt. Express* **2007**, *15*, 14129–14145.
8. Fan, J. A.; Bao, K.; Wu, C.; Bao, J.; Bardhan, R.; Halas, N. J.; Manoharan, V. N.; Shvets, G.; Nordlander, P.; Capasso, F. Fano-Like Interference in Self-Assembled Plasmonic Quadrumer Clusters. *Nano Lett.* **2010**, *10*, 4680–4685.
9. Fan, J. A.; Wu, C.; Bao, K.; Bao, J.; Bardhan, R.; Halas, N. J.; Manoharan, V. N.; Nordlander, P.; Shvets, G.; Capasso, F. Self-Assembled Plasmonic Nanoparticle Clusters. *Science* **2010**, *328*, 1135–1138.
10. Hentschel, M.; Dregely, D.; Vogelgesang, R.; Giessen, H.; Liu, N. Plasmonic Oligomers: The Role of Individual Particles in Collective Behavior. *ACS Nano* **2011**, *5*, 2042–2050.
11. Hentschel, M.; Saliba, M.; Vogelgesang, R.; Giessen, H.; Alivisatos, A. P.; Liu, N. Transition from Isolated to Collective Modes in Plasmonic Oligomers. *Nano Lett.* **2010**, *10*, 2721–2726.
12. Luk'yanchuk, B.; Zheludev, N. I.; Maier, S. A.; Halas, N. J.; Nordlander, P.; Giessen, H.; Chong, C. T. The Fano Resonance in Plasmonic Nanostructures and Metamaterials. *Nat. Mater.* **2010**, *9*, 707–715.
13. Halas, N. J.; Lal, S.; Chang, W.-S.; Link, S.; Nordlander, P. Plasmons in Strongly Coupled Metallic Nanostructures. *Chem. Rev.* **2011**, *111*, 3913–3961.
14. Sonnefraud, Y.; Verellen, N.; Sobhani, H.; Vandenbosch, G. A. E.; Moshchalkov, V. V.; Dorpe, P.; Van; Nordlander, P.; Maier, S. A. Experimental Realization of Subradiant, Superradiant, and Fano Resonances in Ring/Disk Plasmonic Nanocavities. *ACS Nano* **2010**, *4*, 1664–1670.
15. Verellen, N.; Sonnefraud, Y.; Sobhani, H.; Hao, F.; Moshchalkov, V. V.; Dorpe, P.; Van; Nordlander, P.; Maier, S. A. Fano Resonances in Individual Coherent Plasmonic Nanocavities. *Nano Lett.* **2009**, *9*, 1663–1667.
16. Prodan, E.; Radloff, C.; Halas, N. J.; Nordlander, P. A. Hybridization Model for the Plasmon Response of Complex Nanostructures. *Science* **2003**, *302*, 419–422.
17. Haken, H.; Wolf, H. C. *Molecular Physics and Elements of Quantum Chemistry*, 5th ed.; Springer: Berlin, 2003.
18. Fofang, N. T.; Park, T.-H.; Neumann, O.; Mirin, N. A.; Nordlander, P.; Halas, N. J. Plexcitonic Nanoparticles: Plasmon-Exciton Coupling in Nanoshell-J-Aggregate Complexes. *Nano Lett.* **2008**, *8*, 3481–3487.
19. Mirin, N. A.; Bao, K.; Nordlander, P. Fano Resonances in Plasmonic Nanoparticle Aggregates. *J. Phys. Chem. A* **2009**, *113*, 4028–4034.
20. Atkins, P. W.; Paula, J. *Physical Chemistry*, 8th ed.; Oxford University Press: Oxford, 2006.
21. Gómez, D. E.; Vernon, K. C.; Davis, T. J. Symmetry Effects on the Optical Coupling Between Plasmonic Nanoparticles with Applications to Hierarchical Structures. *Phys. Rev. B* **2010**, *81*, 1–10.
22. Lassiter, J. B.; Sobhani, H.; Fan, J. A.; Kundu, J.; Capasso, F.; Nordlander, P.; Halas, N. J. Fano Resonances in Plasmonic Nanoclusters: Geometrical and Chemical Tunability. *Nano Lett.* **2010**, *10*, 3184–3189.
23. Le, F.; Brandl, D. W.; Urzhumov, Y. A.; Wang, H.; Kundu, J.; Halas, N. J.; Aizpurua, J.; Nordlander, P. Metallic Nanoparticle Arrays: A Common Substrate for Both Surface-Enhanced Raman Scattering and Surface-Enhanced Infrared Absorption. *ACS Nano* **2008**, *2*, 707–718.
24. Lee, S. J.; Guan, Z.; Xu, H.; Moskovits, M. Surface-Enhanced Raman Spectroscopy and Nanogeometry: The Plasmonic Origin of SERS. *J. Phys. Chem. C* **2007**, *111*, 17985–17988.
25. Lal, S.; Link, S.; Halas, N. J. Nano-Optics from Sensing to Waveguiding. *Nat. Photonics* **2007**, *1*, 641–648.
26. Liu, N.; Weiss, T.; Mesch, M.; Langguth, L.; Eigenthaler, U.; Hirscher, M.; Sönnichsen, C.; Giessen, H. Planar Metamaterial Analogue of Electromagnetically Induced Transparency for Plasmonic Sensing. *Nano Lett.* **2010**, *10*, 1103–7.
27. Artar, A.; Yanik, A. A.; Altug, H. Directional Double Fano Resonances in Plasmonic Hetero-Oligomers. *Nano Lett.* **2011**, DOI: 10.1021/nl201677h.
28. Neubrech, F.; Pucci, A.; Cornelius, T.; Karim, S.; García-Etxarri, A.; Aizpurua, J. Resonant Plasmonic and Vibrational Coupling in a Tailored Nanoantenna for Infrared Detection. *Phys. Rev. Lett.* **2008**, *101*, 157403.
29. Maier, S. A.; Kik, P. G.; Atwater, H. A.; Meltzer, S.; Harel, E.; Koel, B. E.; Requicha, A. A. G. Local Detection of Electromagnetic Energy Transport below the Diffraction Limit in Metal Nanoparticle Plasmon Waveguides. *Nat. Mater.* **2003**, *2*, 229–232.
30. Maier, S. A.; Brongersma, M. L.; Kik, P. G.; Meltzer, S.; Requicha, A. A. G.; Atwater, H. A. Plasmonics—A Route to Nanoscale Optical Devices. *Adv. Mater.* **2001**, *13*, 1501.
31. Liu, N.; Langguth, L.; Weiss, T.; Kästel, J.; Fleischhauer, M.; Pfau, T.; Giessen, H. Plasmonic Analogue of Electromagnetically Induced Transparency at the Drude Damping Limit. *Nat. Mater.* **2009**, *8*, 758–762.
32. Bao, K.; Mirin, N. A.; Nordlander, P. Fano Resonances in Planar Silver Nanosphere Clusters. *Appl. Phys. A: Mater. Sci. Process.* **2010**, *100*, 333–339.
33. Huang, J.-S.; Callegari, V.; Geisler, P.; Brüning, C.; Kern, J.; Prangsma, J. C.; Wu, X.; Feichtner, T.; Ziegler, J.; Weinmann, P.; *et al.* Atomically Flat Single-Crystalline Gold Nanostructures for Plasmonic Nanocircuitry. *Nat. Commun.* **2010**, *1*, 150.
34. Duan, H.; Hu, H.; Kumar, K.; Shen, Z.; Yang, J. K. W. The Direct and Reliable Patterning of Plasmonic Nanostructures with Sub-10-nm Gaps. *ACS Nano* **2011**, DOI: 10.1021/nn2025868.

35. Engheta, N. Circuits with Light at Nanoscales: Optical Nanocircuits Inspired by Metamaterials. *Science* **2008**, *317*, 1698–1702.
36. Engheta, N.; Salandrino, A.; Alù, A. Circuit Elements at Optical Frequencies: Nanoinductors, Nanocapacitors, and Nanoresistors. *Phys. Rev. Lett.* **2005**, 95.
37. Oulton, R. F.; Sorger, V. J.; Zentgraf, T.; Ma, R.-M.; Gladden, C.; Dai, L.; Bartal, G.; Zhang, X. Plasmon Lasers at Deep Subwavelength Scale. *Nature* **2009**, *461*, 629–632.
38. Stockman, M. Dark-Hot Resonances. *Nature* **2010**, *467*, 541–542.
39. Yan, B.; Thubagere, A.; Premasiri, W. R.; Ziegler, L. D.; Negro Dal, L.; Reinhard, B. M. Engineered SERS Substrates with Multiscale Signal Enhancement: Nanoparticle Cluster Arrays. *ACS Nano* **2009**, *3*, 1190–1202.
40. Baciu, C. L.; Becker, J.; Janshoff, A.; Sönnichsen, C. Protein-Membrane Interaction Probed by Single Plasmonic Nanoparticles. *Nano Lett.* **2008**, *8*, 1724–1728.
41. Kim, S.; Jin, J.; Kim, Y.-J.; Park, I.-Y.; Kim, Y.; Kim, S.-W. High-Harmonic Generation by Resonant Plasmon Field Enhancement. *Nature* **2008**, *453*, 757–760.
42. Johnson, P.; Christy, R. Optical Constants of the Noble Metals. *Phys. Rev. B* **1972**, *6*, 4370–4379.